JOURNAL OF CATALYSIS **161,** 783–789 (1996)
ARTICLE NO. 0241

Use of Mesoporous MCM-41 Aluminosilicates as Catalysts in the Production of Fine Chemicals: Preparation of Dimethylacetals

M. J. Climent, A. Corma,[1] S. Iborra, M. C. Navarro, and J. Primo

Departamento de Química, Instituto de Tecnología Química (UPV–CSIC), Avenida de Los Naranjos s/n, 46022 Valencia, Spain

Received December 18, 1995; revised March 19, 1996; accepted March 20, 1996

Dimethylacetals have been prepared by reacting aldehydes with trimethyl orthoformate. Large pore zeolites (HY and beta) as well as mesoporous silica–aluminas with regular pore sizes, such as MCM-41 and SAM, and commercial amorphous silica–alumina with a broader distribution of pore sizes have been used as catalysts. The results indicate that in addition to bridging hydroxyl groups, silanols can also be active for carrying out this reaction. Zeolites are more active than the mesoporous materials, but their activity decays faster. By carrying out the reaction with aldehydes of different molecular sizes it is shown that the MCM-41 mesoporous materials are promising catalysts for their use in the production of fine chemicals which involve bulky reactants or products. Finally, mesoporous catalysts with a very narrow pore size distribution show a better catalytic behavior than others with a broader pore size distribution. © 1996 Academic Press, Inc.

INTRODUCTION

The discovery by Kresge *et al.* (1) of new mesoporous aluminosilicates of the M41-S family with regular pore dimensions which can be varied between 20 and 100 Å opened new possibilities in the field of solid acid catalysis. The obvious first attempt of application was in FCC catalysts, but the limited hydrothermal stability of these materials makes their use in actual FCC units problematic (2). However, they appear promising for preparation of hydrocracking catalysts (3) since they can work with milder acidities and hydrothermal stabilities than those needed for FCC. Indeed, it has been stablished that the acid strength of these aluminosilicates is similar to that of amorphous silica–alumina and in any case their acidity is much weaker than in zeolites (4). Therefore, it appears that the best possibilities for these materials in catalysis will be in processes needing moderate acidity and involving bulky size molecules. Thus, one field which can take advantage of the properties of the MCM-41 is the preparation of fine chemicals, and more specifically, the catalytic preparation of acetals. These compounds are interesting from an industrial point of view for their use in pharmaceuticals (5, 6) and as fragrances in perfumes and detergents (7). The preparation of acetals by acid catalysis does not require strong acid sites and many of them are too bulky to diffuse through the pores of zeolites. Therefore, it can be expected that the new mesoporous aluminosilicates can be adequate catalysts for carrying out acetalization reactions.

In the present work we have studied the catalytic possibilities of two types of mesoporous aluminosilicates for preparation of dimethylacetals using trimethyl orthoformate (TOF) as reactant. One of them, MCM-41, has a hexagonal arrangement of pores of 35 Å. The other, SAM (8), is completely amorphous, but presents a narrow distribution of pores centered around 15 Å. Their activity and selectivity for the preparation of dimethylacetals with different molecular sizes will be compared with those of large pore zeolites and classical amorphous silica–alumina.

EXPERIMENTAL

Catalysts

The HY-100 zeolite was prepared starting from a commercial NaY sample (SK-40, Union Carbide) with a 0.25 *M* aqueous solution of ammonium acetate using a solid–liquid weight ratio of 1 : 4 at 298 K for 30 min. The resulting zeolite was dried at 383 K for 6 h and deep-bed calcined at 823 K for 3 h. This partially exchanged Y zeolite was submitted to two additional exchange–calcination treatments as above using successively 0.40 and 0.60 *M* solutions of ammonium acetate. The average crystal size of SK-40, as determined by scanning electron microscopy (SEM), was 0.8 μm, and the framework Si/Al ratio of the resultant HY-100 zeolite was 4.5.

Hβ zeolites were prepared starting from a TEA-β (9) (Si/Al = 13) by heating at 773 K in a N_2 stream followed by calcination in air at 823 K and twice NH_4^+ exchanged and calcined at 823 K.

The amorphous silica–alumina with regular pores was named as SAM and prepared according with Ref. (8).

Mesoporous materials MCM-41 were synthesized following the procedure given in Ref. (10) using hexadecyl-

---

[1] To whom correspondence should be addressed. Fax: 96-387 78 09.

0021-9517/96 $18.00

TABLE 1

Main Structural Characteristics of the Catalysts

Catalysts	Surface area ($m^2\ g^{-1}$)	Pore[a] volume ($cm^3\ g^{-1}$)	Si/Al	Average[b] pore diameter (Å)
1-MCM-41	900	0.500	14.0	35
2-MCM-41	837	0.480	83.0	34
SAM	719	0.310	50.0	15
Silica–alumina	268	0.282	2.5	24
HY	709	0.323	4.5	7.4
Hβ	607	0.175	13.0	$7.6 * 6.4$ $5.5 * 5.5$

[a] Measured by N_2.
[b] Measured by Ar.

trimethylammonium (Aldrich) cation as template, and pseudobohemite (Capatal B, Vista) and Aerosil (Gussa) as the aluminum and silicon source, respectively. The samples were activated by calcination in N_2 for 1 h and in air for 6 h at 813 K.

A commercial sample of amorphous silica–alumina (25 wt% Al_2O_3) was supplied by Crosfield.

The main characteristics of the samples used are summarized in Table 1.

The solids were characterized by X-ray diffraction on a Phillips PW diffractometer using Cu$K\alpha$ radiation. Surface area measurements were obtained on an ASAP-2000 apparatus following the BET procedure. Pore diameter distribution was obtained using argon as adsorbate and following the Horvath–Kawazoe method (11). IR spectra were recorded on a Nicolet 710 FTIR spectrophotometer, using 10 mg cm^{-2} wafers of the samples treated in a vacuum cell at 673 K for 16 h. Pyridine was then admitted at room temperature and, after saturation, the samples were degassed at 423, 523, and 673 K, and IR spectra were recorded.

Reaction Procedure

Activation of the catalyst was performed *in situ* by heating the solid under vacuum (1 Torr) for 3 h. After this time, the system was left at room temperature and then a solution of the carbonyl compound (technical grade, from Aldrich) (3 mmol) and TOF (98%, from Aldrich) (15 mmol) in tetrachloromethane (technical grade, from Panreac) (25 ml) as solvent was poured onto the activated catalyst. The resulting suspension was magnetically stirred at reflux temperature for 5 h. At the end of the reaction the catalyst was filtered and washed with dichloromethane. The organic solution was concentrated in vacuum, and the residue was weighed and analyzed by gas chromatography–mass spectrometry (GC–MS) using a Hewlett-Packard 5988A spectrometer provided with a 25-m capillary column of cross-linked 5% phenylmethylsilicone; the ratios m/z and the relative intensities (%) are indicated for the significant peaks. After reaction, the catalysts were submitted to continuous solid–liquid extraction with dichloromethane using a micro-Soxhlet equipment. After removal of the solvent the residue was also weighed and analyzed by GC–MS and ^{1}H NMR spectroscopy. In all cases the recovered material accounted for more than 90% of the starting material. The ^{1}H NMR analysis of the products was carried out with a 400 MHz Varian VXR-400 S spectrometer in deuterated trichloromethane and TMS as internal standard; chemical shifts are reported in δ (ppm) referenced to TMS.

Spectroscopic Data of the Reaction Products

1,1-Dimethoxyheptane (**1a**): ^{1}H NMR, 4.33 (t, 1H, $C\underline{H}(OCH_3)_2$), 3.24 (s, 6H, $2OC\underline{H}_3$), 1.51 (m, 2H, $C\underline{H}_2{-}CH{-}(OCH_3)_2$), 1.22 (m, 8H, $4C\underline{H}_2$), 0.83 (t, 3H, $C\underline{H}_3$); MS: 159 (M^+-1, 3), 129(100), 97(3), 75(16).

1,1-Dimethoxy-2-phenylpropane (**2a**): ^{1}H NMR, 7.40–7.00 (m, 5H, Ar$\underline{H}$), 4.30 (d, $J = 8$ Hz, 1H, $C\underline{H}{-}(OCH_3)_2$), 3.37 (s, 3H, $OC\underline{H}_3$), 3.15 (s, 3H, $OC\underline{H}_3$), 2.85 (m, 1H, Ph$-$C$\underline{H}$), 1.20 (d, $J = 8$ Hz, $C\underline{H}_3$); MS: 179 (M^+-1, 1), 149(56), 117(35), 105(54), 77(38), 75(100).

(E)-1-Methoxy-2-phenylpropene (**2b**): ^{1}H NMR, 7.60–6.90 (m, 5H, Ar$\underline{H}$), 6.30 (q, $J = 1.5$ Hz, 1H, $CH{-}OC\underline{H}_3$), 3.59 (s, 3H, $OC\underline{H}_3$), 1.92 (d, $J = 1.5$ Hz, 3H, $C\underline{H}_3$); MS: 148 (M^+, 75), 133(15), 115(10), 105(100), 103(22), 91(7).

1,1-Dimethoxy-2,2-diphenylethane (**3a**): ^{1}H NMR, 7.80–7.19 (m, 10H, Ar$\underline{H}$), 5.00 (d, $J = 8$ Hz, 1H, $C\underline{H}(Ph)_2$), 4.25 (d, $J = 8$ Hz, 1H, $C\underline{H}(OCH_3)_2$), 3.30 (s, 6H, $2OC\underline{H}_3$); MS: 241(M^+-1, 1), 211(100), 167(18), 165(33), 152(14), 105(13), 75(66).

1-Methoxy-2,2-diphenylethene (**3b**): ^{1}H NMR, 7.75–7.20 (m, 10H, Ar$\underline{H}$), 6.45 (s, 1H, $C{=}C\underline{H}$), 3.79 (s, 3H, $OC\underline{H}_3$); MS: 210(M^+, 100), 195(12), 167(40), 165(15).

RESULTS AND DISCUSSION

Three aldehydes of different molecular sizes, heptanal (**1**), 2-phenylpropanal (**2**), and diphenylacetaldehyde (**3**) were reacted with TOF to produce the corresponding dimethylacetals.

When the transacetalization of **2** was carried out on the 1-MCM-41 catalyst, both the corresponding dimethylacetal **2a** and the enol ether **2b** were produced (Scheme 1).

The kinetic results presented in Fig. 1 show that good yields and selectivities of **2a** are obtained at reaction times of 2 h. Moreover, **2a** appears as a primary product, while **2b** can be primary plus secondary product. The product behavior observed can be explained from the reaction mechanism given in Scheme 2.

In this mechanism the carbocationic species (I) is the common intermediate for producing **2a** and **2b**, and in the presence of excess methanol and a fair concentration of acid sites, the equilibrium should be shifted by protonation of **2b** to produce more stable **2a**. However, from the results

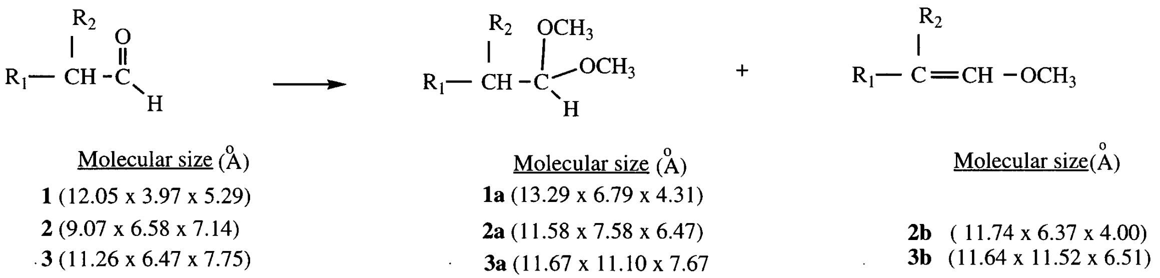

	R_1	R_2
1	$CH_3(CH_2)_4$	H
2	Ph	CH_3
3	Ph	Ph

SCHEME 1

of Fig. 1, the possibility that at high concentrations (after 2 h reaction time), **2a** could react back to give **2b** through the common intermediate (I) cannot be ruled out.

The catalyst active sites involved in the reaction were thought to be acid sites related to bridging hydroxyl groups, which in the case of the MCM-41 sample should be related to the presence of tetrahedrally coordinated Al in the amorphous walls which delimit the channels in the MCM-41 structure. Then, the hydroxyls associated with this Al^{IV} should be responsible for the Brønsted acidity necessary to catalyze the reaction. Indeed, the Al^{27} MAS NMR analysis of the sample (4) showed that only Al^{IV} could be observed in the synthesized sample before calcination. After calcining the sample for activation, there was still Al^{IV}, even though part of the original Al^{IV} are transformed into Al^{VI}. The presence of the Brønsted acidity associated with the remaining Al^{IV} has been determined by pyridine adsorption (Fig. 2A). The presence of a pyridinium band at 1545 cm^{-1} indicates the presence in the 1-MCM-41 sample of Brønsted acid sites able to protonate pyridine that remains adsorbed after evacuation at 423 K. The 1455 cm^{-1} band corresponds to pyridine coordinated to Lewis acid sites, probably related with the presence of Al^{VI} generated after calcination.

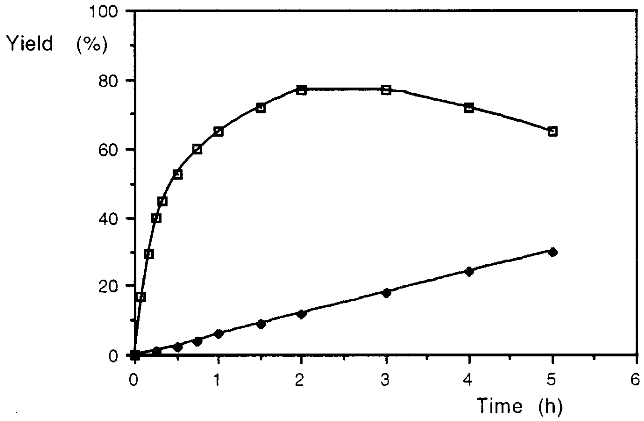

FIG. 1. Yield (%) of dimethylacetal **2a** (□) and the enol ether **2b** (◆) versus the reaction time when **2** (0.402 g, 3 mmol) and TOF (1.59 g, 15 mmol) is heated in CCl_4 (25 ml) at 351 K over 1-MCM-41.

If one accepts that the acid Brønsted sites associated to tetrahedrally coordinated Al (Si–OH–Al) are the only active ones for the formation of acetals, then the activity of MCM-41 samples should be directly proportional to the Al^{IV} content. Following this, the 2-MCM-41 sample which has a much lower Al^{IV} content, a lower amount of Brønsted acid sites measured by pyridine adsorption (Fig. 2B), and a similar surface area to 1-MCM-41 should give a much lower catalytic activity. However, the results given in Table 2 clearly show that the initial reaction rate on 2-MCM-41 is not smaller than on 1-MCM-41. Therefore, we must conclude that bridging hydroxyl groups (Si–OH–Al) are not the only active groups for catalyzing the acetalization reaction, but other weaker acid sites such as silanols, or at least silanol groups in the neighborhood of Al^{IV}, can be acid enough to catalyze the acetalization reaction. Nevertheless, one may expect the intrinsic activity of the bridging hydroxyl groups to be higher than the activity of the less acidic silanol groups. The IR results in the hydroxyl region (Fig. 3) clearly show that MCM-41 samples have a very large amount of silanol groups, being the population larger on the 2-MCM-41. This would explain the observed differences in catalytic activity.

The hypothesis presented above is consistent with the observation that the activity obtained on an amorphous silica–alumina (SAM) with a Si/Al ratio of 50, a narrow pore size distribution, and with a similar surface area to the MCM-41 samples (Fig. 4), shows practically the same catalytic activity for the acetalization of **2** as MCM-41 samples.

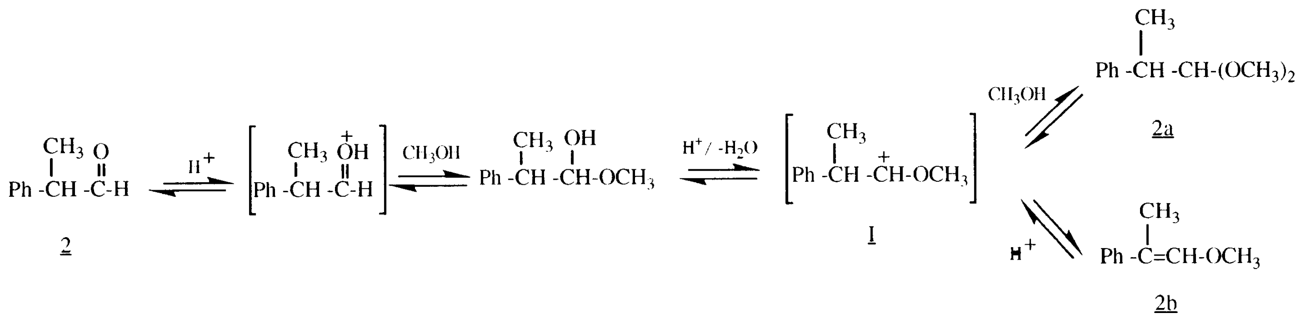

SCHEME 2

This observation is in agreement with the results presented by Bellusi *et al.* (12) for the oligomerization of olefins, a reaction requiring acid sites of low strength, and which gives similar conversions on MCM-41 and SAM.

For comparative purposes, we have compared the results obtained on MCM-41 materials with those obtained on two types of aluminosilicates: amorphous silica–alumina and zeolites. Amorphous silica–alumina, while being active for formation of acetals, is less active than MCM-41 materials and we relate this difference, with the larger surface area presented by the MCM-41 catalysts. In the case of zeolites, the two large pore zeolites studied here (HY and beta), are quite active catalysts for acetalization, their activity being larger than that of MCM-41 samples. In order to explain

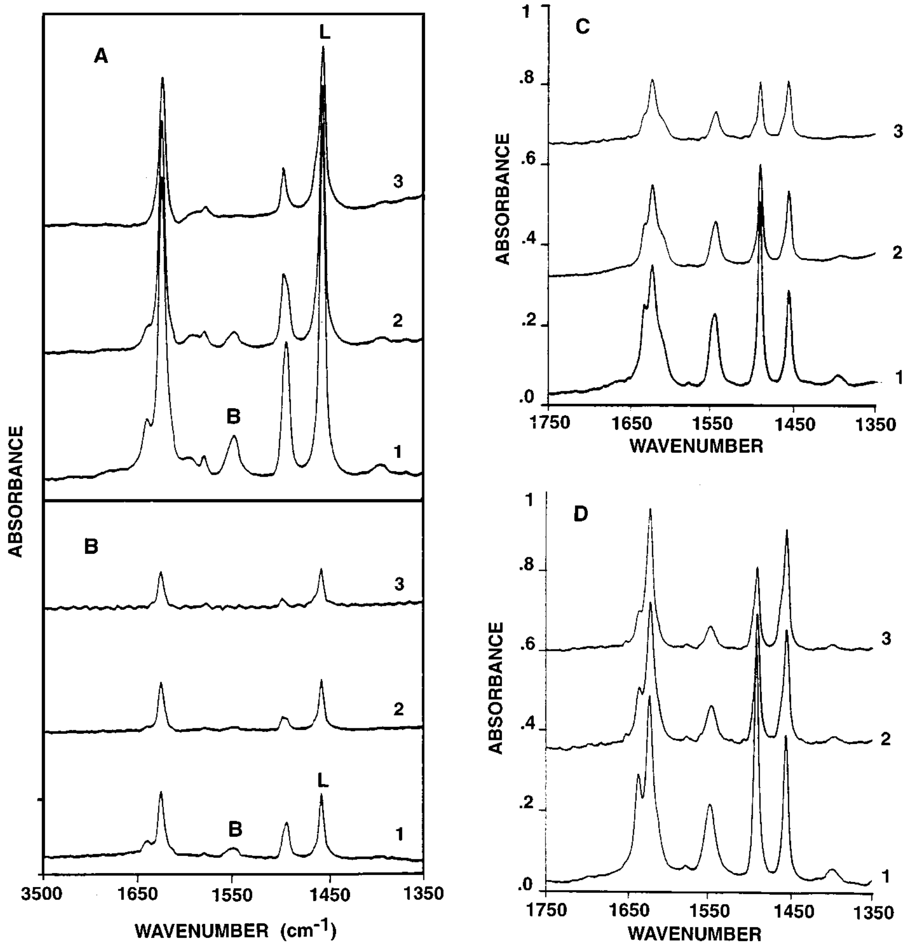

FIG. 2. IR spectra of pyridine adsorbed on (A) 1-MCM-41 sample, (B) 2-MCM-41 after different desorption treatments: (1) 423 K, (2) 573 K, (3) 673 K. (C) HY and (D) Hβ after different desorption treatments: (1) 525 K, (2) 623 K, (3) 673 K.

TABLE 2

Initial Rates and Yields of the Acetalization of 2 on Different Acid Catalysts

Catalysts	r_o (mol h^{-1} g^{-1}) × 10^3	Selectivity (%)[a] **2a**	Yield (%)[a] **2a**	**2b**
1-MCM-41	2480	87	79	11
2-MCM-41	3040	92	91	8
SAM	2420	93	85	6
SiO_2/Al_2O_3	1600	91	70	7
HY	6540	93	89	7
βH	4080	92	86	8

[a] 2 h reaction time.

these results we must conclude that the bridging hydroxyl groups present in much larger amounts in zeolites (Figs. 2C and 2D) than in MCM-41 have a higher intrinsic activity than the weaker acid sites related to silanol groups. Thus, it appears that when the reactants can diffuse inside the pores of zeolites, the microporous materials are more active than the mesoporous MCM-41 and SAM samples.

Influence of the Size of Reactant

The influence of the catalyst pore size on the activity for carrying out the acetalization of aldehydes with different kinetic diameter, *n*-heptanal (**1**), 2-phenylpropanal (**2**), and diphenylacetaldehyde (**3**) is shown from the results given in Table 3. The molecular size of the different reactants and products have been measured using a molecular docking simulations (13) and are included in Scheme 1.

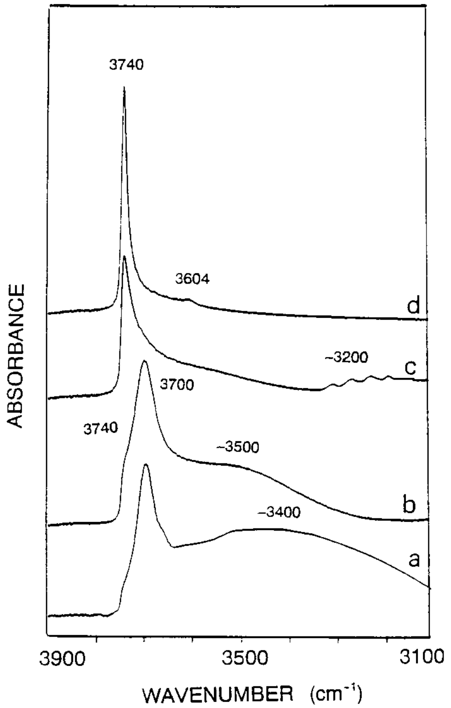

FIG. 3. IR spectra in the hydroxyl range of 1-MCM-41 after different thermal treatments: calcination in vacuum 1 h at (a) 423 K, (b) 573 K, (c) 673 K, and (d) 773 K.

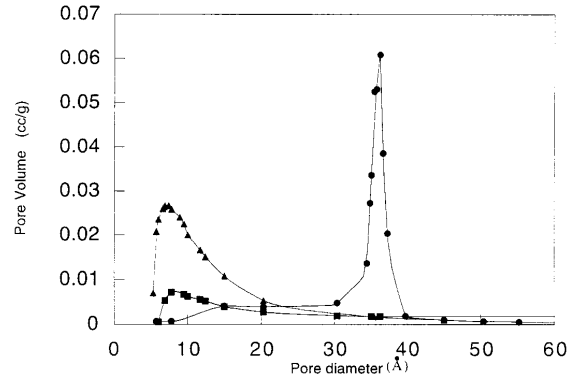

FIG. 4. Pore size distribution of SAM (▲), 1-MCM-41 (●), and silica–alumina (■).

In the case of the MCM-41 samples it is possible to see that the initial rate of reaction is very similar regardless of the size of the reactant aldehyde. On the other hand, the catalytic activity of the zeolite catalysts decreases when increasing the size of the reactant. This reduction is especially remarkable for the acetalization of diphenylacetaldehyde (**3**) which should be strongly impeded to diffuse in the pores as well as the bulkier reaction products to diffuse out of the zeolite pores. This was checked by studying the influence of the zeolite crystal sizes on the conversion of the three aldehydes. Two beta zeolite samples with crystal size of 0.06 μm (1-βH) and 0.86 μm (2-βH) were used and the results are shown in Table 3. It can be seen that in the case of the smallest reactant molecule, i.e., heptanal (**1**), there is very little influence of the zeolite crystal size on the initial rate of the reaction. However, when 2-phenylpropanal (**2**) was reacted, a decrease in conversion is observed on both beta zeolites samples, this decrease being larger for the zeolite with bigger crystallites. A dramatic decrease in activity on both samples is observed when reacting diphenylacetalde-

TABLE 3

Influence of the Catalyst Pore Size on the Rate and Conversion in the Acetalization Reaction of 1, 2, and 3

	r_o (mol h^{-1} g^{-1}) × 10^3			Conversion (%)[a]		
Catalysts	**1**	**2**	**3**	**1**	**2**	**3**
1-MCM-41	2500	2480	2340	98	90	80
1-βH	3300	2180	380	89	83	13
2-βH	3080	1340	180	94	55	8

[a] 2 h reaction time.

hyde (**3**), in any case the decrease being larger for the zeolite with larger crystal sizes.

From the point of view of the catalytic activity of the different mesoporous materials studied here, results from Table 4 are quite instructive. Indeed, the catalytic activity of the classical amorphous silica–alumina and SAM material decreases when increasing the size of the reactant aldehyde. On the other hand, the activity of the MCM-41 sample is practically the same regardless the size of the aldehyde sample studied here. It appears from these results that in the former material there is a larger distribution of pore sizes, a fraction of them being in the microporous region and therefore limiting the diffusivity of the larger diphenylacetaldehyde (**3**). In the case of MCM-41 structure the highly regular size of the pores with diameter large enough to allow the diffusion of any of the three aldehydes show practically no differences on reactivity toward the nature of the reactant.

Concerning catalyst deactivation, results from Figs. 5a–5b show that for reactants **1** and **2**, little deactivation is observed with either zeolite HY or the 2-MCM-41 sample. However, for reactant **3**, it is possible to see that on zeolite HY the conversion stops at 55%, and on the other hand, 2-MCM-41, while having practically the same initial activity, can achieve a final larger conversion (Fig. 5c). This can be an indication that the large products formed with reactant **3** can adsorb in zeolite Y blocking the pores and/or the active sites leading to a loss of catalytic activity. Indeed, after the reaction, the HY and 2-MCM-41 catalysts were subject to continuous solid–liquid extraction with dichloromethane using a micro-Soxhlet equipment. The amounts adsorbed on the catalysts were 1.6 and 1.1 g/g for the micro- and mesoporous materials, respectively.

The extracted samples were again used as catalysts in a second experiment and the loss of the activity (initial rate) found for the HY was 60%, while for 2-MCM-41 it was 40%. Furthermore, the results from Fig. 6 show that after 2 h reaction time, the reused MCM-41 sample achieves practically the same conversion as freshly catalyst, i.e., 90%, while with HY the conversion stops at 32%. In any case, the catalysts can be completed regenerated by calcination in air for 6 h at 673 K.

TABLE 4

Rates of Acetalization of Aldehydes 1, 2, and 3 Using MCM-41, SAM, and Amorphous Silica-Alumina as Acid Catalysts

	r_o (mol h^{-1} g^{-1}) × 10^3		
Catalysts	**1**	**2**	**3**
1-MCM-41	2500	2480	2340
SAM	3800	2420	800
SiO_2/Al_2O_3	1500	1600	460

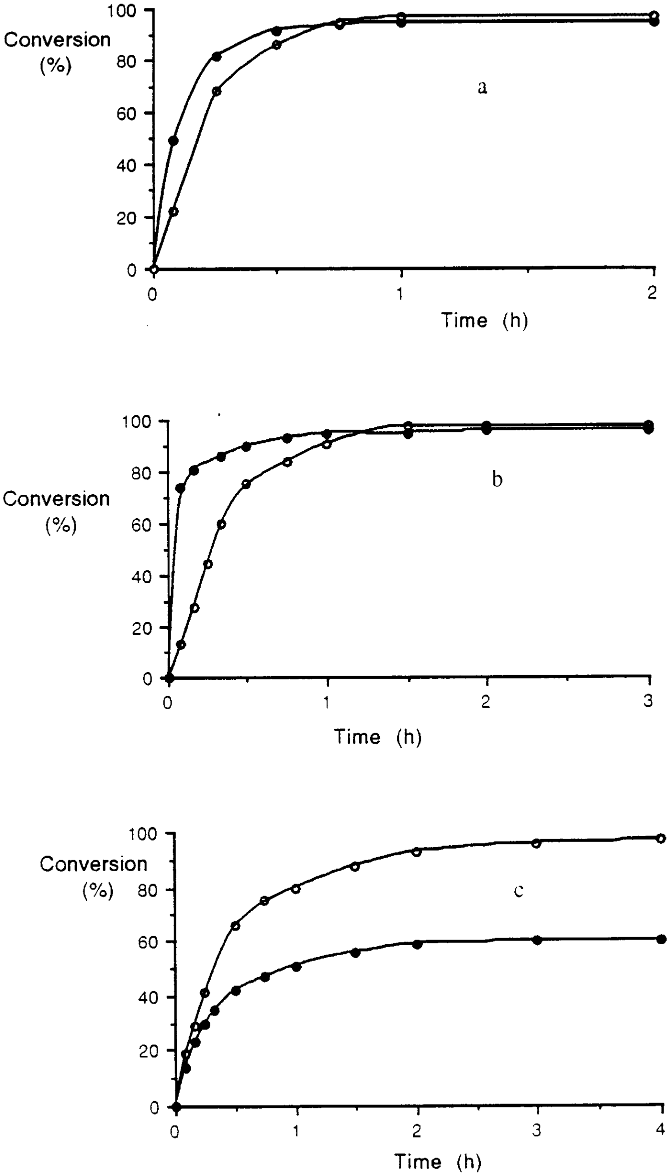

FIG. 5. Conversion total (%) versus the reaction time when the acetalization was carring out using (a) **1**, (b) **2**, and (c) **3** on 2-MCM-41 (○) and HY (●).

The catalyst deactivation results indicate that while zeolites are intrinsically more active catalysts than mesoporous MCM-41 materials for carrying out acetalization reactions, they deactivate more rapidly than mesoporous materials owing to the larger absorption and lower diffusion rates of the reaction products in the microporous structures.

CONCLUSIONS

It has been presented that MCM-41 as well as SAM materials are active and selective catalysts for the acetalization of aldehydes. This reaction requires catalytic sites with

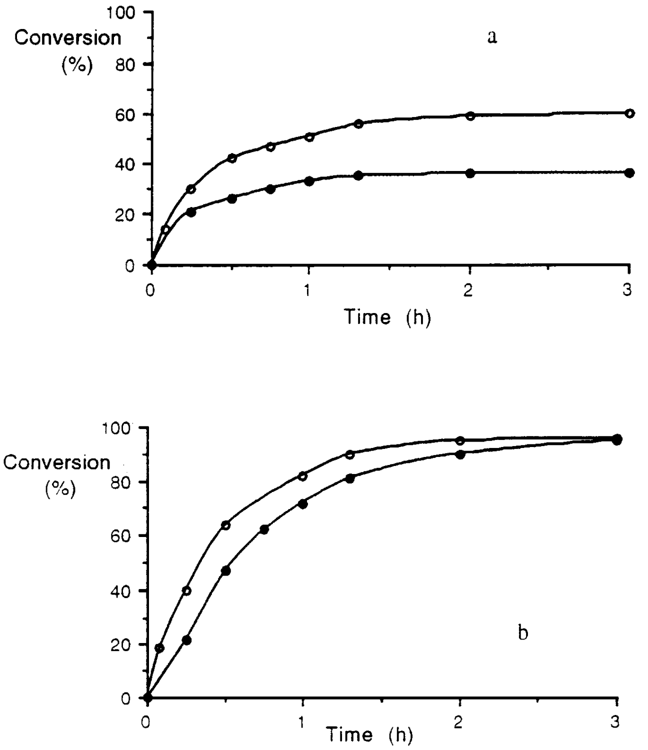

FIG. 6. Catalysis by (a) HY and (b) 2-MCM41 of the acetalization of **3** at 351 K: (○) conversion of **3** of first cycle; (●) conversion of **3** of second cycle.

low acid strength and it appears that in additon to bridging hydroxyl groups, silanol groups could also be active.

It appears that when working with small size aldehydes as reactants, zeolites are intrinsically more active than the mesoporous materials. However, when reactants with sizes larger than 7 Å are used, as is commonly done in the field of fine chemicals, geometrical constraints do not allow the reactants to diffuse inside the pore of the zeolites and only the external surface area of the these materials becomes available to the reactants. In these circumstances the large pores of the MCM-41 make this material more adequate for carrying out acetalization reactions. Moreover, even in the case of smaller reactants, the catalyst decay during formation of acetals is larger on zeolites than on MCM-41 probably due to the higher adsorption and lower rates of diffusion for products on the former. This gives one additional advantage to MCM-41 for its use as acetalization catalysts.

Our results show, for the first time, the benefits derived from the existence of a unique and regularly arranged system of pores in mesoporous amorphous acid solids toward catalytic conversion of bulky reactants. In this sense MCM-41 shows a better catalytic performance than either SAM or classical amorphous silica–alumina for the acetalization of aldehydes of increasing size.

ACKNOWLEDGMENT

Financial support by the Direccion General de Investigacion Científica y Técnica of Spain (Project MAT 94-1035) and European Network (Ref. ERB 4050 PL-932451) is gratefully acknowledged.

REFERENCES

1. Kresge, C. T., Leonowicz, M. E., Roth, W. J., Vartuli, J. C., and BecK, J. S., *Nature* **359**, 710 (1992).
2. Corma, A., Grande, M., and Orchillés, V., *J. Catal.,* in press (1996).
3. Corma, A., Martínez-Soria, A., and Monton, J. B., *J. Catal.* **153**, 25 (1995).
4. Corma, A., Fornés, V., Navarro, M. T., and Pérez-Pariente, J., *J. Catal.* **148**, 569 (1994).
5. Godefroi, E. F., and Meeres, J., U.S. Patent 3,575,999, 1971.
6. Walker, K. A. M., U.S. Patent 4,150,153, 1979.
7. Bauer, K., Garbe, D., and Surburg, H., "Common Fragances and Flavors Materials," 2nd ed., VCH, Weinheim/New York, 1990.
8. Bellusi, G., Perego, C., Carati, A., Peratello, S., Previde Massara, E., and Perego, G., *Stud. Surf. Sci. Catal.* **84**, 85 (1994).
9. Bonetto, L., Camblor, M. A., Corma, A., and Perez-Pariente, J., *Appl. Catal.* **82**, 37 (1992).
10. Beck, J. S., Chu, C., Johnson, J. D., Kresge, C. T., Leonowicz, M. E., Roth, W. J., and Vartuli, J. C., WO 9,111,390, 1992.
11. Horvath, G., and Kawazoe, K., *J. Chem. Eng. Jpn.* **16**, 470 (1983).
12. Bellusi, G., Cavani, F., Arrigoni, V., and Ghezzi, R., European Patent 463,673, 1992.
13. Docking using the Biosym Inside II Molecular Modeling package running on a Silicon Graphics workstation.